**Atmospheric
Chemistry
and Physics
Discussions**

Night-time chemistry above London: measurements of NO_3 and N_2O_5 from the BT Tower during REPARTEE-II

A. K. Benton[1], J. M. Langridge[1,*], S. M. Ball[2], W. J. Bloss[3], M. Dall'Osto[3,**],
E. Nemitz[4], R. M. Harrison[3], and R. L. Jones[1]

[1]Centre for Atmospheric Science, Department of Chemistry, University of Cambridge,
Lensfield Road, Cambridge, CB2 1EW, UK
[2]Department of Chemistry, University of Leicester, University Road, Leicester, LE1 7RH, UK
[3]National Centre for Atmospheric Science, School of Geography, Earth and Environmental
Sciences, University of Birmingham, Birmingham, B15 2TT, UK
[4]Centre for Ecology and Hydrology (Edinburgh), Bush Estate, EH26 0QB, Penicuik, UK
[*]now at: Cooperative Institute for Research in Environmental Sciences (CIRES), University of
Colorado at Boulder, and NOAA Earth System Research Laboratory (ESRL), Boulder,
Colorado, USA

Discussion Paper | Discussion Paper | Discussion Paper | Discussion Paper

ACPD

10, 14347–14386, 2010

**Night-time chemistry
above London**

A. K. Benton et al.

Title Page

Abstract	Introduction
Conclusions	References
Tables	Figures

|◄ | ►|
◄ | ►

Back | Close

Full Screen / Esc

Printer-friendly Version

Interactive Discussion

**now at: School of Physics and Centre for Climate and Air Pollution Studies, Environmental Change Institute National University of Ireland, Galway, Ireland

Correspondence to: A. K. Benton (akb36@cam.ac.uk)

Night-time chemistry above London

A. K. Benton et al.

Abstract

Broadband cavity enhanced absorption spectroscopy (BBCEAS) has been used to measure the sum of concentrations of NO_3 and N_2O_5 from the BT (telecommunications) Tower 160 m above street level in central London during the REPARTEE II campaign in October and November 2007. Substantial variability was observed in these night-time nitrogen compounds: peak $NO_3+N_2O_5$ mixing ratios reached 800 pptv, whereas the mean night-time $NO_3+N_2O_5$ was approximately 30 pptv. Additionally, $[NO_3+N_2O_5]$ showed negative correlations with $[NO]$ and $[NO_2]$ and a positive correlation with $[O_3]$. Co-measurements of temperature and NO_2 from the BT Tower were used to calculate the equilibrium partitioning between NO_3 and N_2O_5 which was always found to strongly favour N_2O_5 (NO_3/N_2O_5=0.01 to 0.04). Two methods are used to calculate the lifetimes for NO_3 and N_2O_5, the results being compared and discussed in terms of the implications for the night-time oxidation of nitrogen oxides and the night-time sinks for NO_y.

1 Introduction

The nitrate radical (NO_3) is amongst the most important oxidants in the nocturnal boundary layer (NBL). It is responsible for initiating the processing of a wide range of anthropogenic and biogenic emissions and in many ways can be considered the night-time analogue of the hydroxyl radical. Understanding the atmospheric cycle of NO_3 – its formation and loss pathways, spatial variability, and role in the regulation of NO_x($NO+NO_2$) and budgets of volatile organic compounds (VOCs) (Atkinson, 2000), is of key importance to understanding processes impacting surface ozone formation and air quality.

1.1 Chemistry of NO_3 and N_2O_5

Figure 1 shows a simplified scheme of nocturnal nitrogen oxide chemistry. NO_2 is formed from NO (R1), which has a predominant traffic source. NO_2 and O_3 react to form NO_3, (R2) which further reacts with NO_2. During night-time, N_2O_5 can be formed through reaction of NO_2 and NO_3(R3).

$$NO + O_3 \rightarrow NO_2 + O_2 \qquad\qquad k_1 \qquad\qquad\qquad (R1)$$
$$NO_2 + O_3 \rightarrow NO_3 + O_2 \qquad\qquad k_2 \qquad\qquad\qquad (R2)$$
$$NO_2 + NO_3 + M \leftrightarrow N_2O_5 + M \qquad\quad k_3 \qquad\qquad\qquad (R3)$$
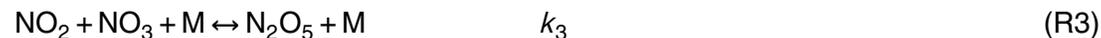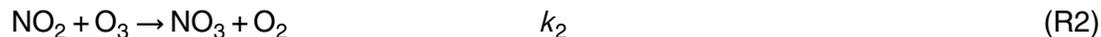
At night NO_3 and N_2O_5 exist in a temperature dependent equilibrium (Wangberg et al., 1997) which is established within minutes under typical atmospheric conditions (Brown, 2003). The major sinks for NO_3 are solar photolysis (Stark et al., 2007) which effectively suppresses NO_3 and N_2O_5 concentrations during daylight hours, and the extremely fast reaction with NO (Hammer et al., 1986).

In addition to gas phase sinks, the heterogeneous conversion of N_2O_5 to aqueous nitrate (R4) provides an effective pathway for removal of NO_x from the atmosphere (Dentener and Crutzen, 1993; Brown et al., 2004). Despite universal recognition of the importance of this process, its global influence remains relatively poorly quantified, in large part due to the complexity of the dependence of N_2O_5 uptake on aerosol chemical composition and mixing state (Mentel et al., 1996; Hallquist et al., 2000). Recent investigations have found that night-time removal of NO_y (=all oxides of nitrogen) via the above channels can be almost as effective at removing NO_y from the atmosphere as the major daytime pathway proceeding via the reaction of OH with NO_2 (Brown et al., 2007a,b).

$$N_2O_5 + H_2O_{(l)} \xrightarrow{\text{heterogeneous}} 2HNO_3 \qquad\quad k_{\text{het}} \qquad\qquad\qquad (R4)$$

Night-time chemistry above London

A. K. Benton et al.

1.2 Vertical extent of NO_3 and N_2O_5 structure

A number of factors lead to pronounced vertical structure of N_2O_5 and NO_3 in the nocturnal boundary layer. NO sources are generally located at the ground surface and act to suppress both local NO_3 and O_3 concentrations through reaction (R1) and subsequent loss of O_3 source for reaction (R2). Upon ascent through the atmosphere, O_3 levels increase and there is gradual conversion of NO to NO_2 followed by NO_3 and N_2O_5. The absence of significant sinks for NO_3 and N_2O_5 aloft enables significant concentrations of these species to grow, leading to distinct positive vertical concentration gradients.

Meteorological conditions also play a role in establishing vertical gradients. The absence of convection from the surface at night decreases turbulent mixing and leads to a highly stratified, stable layer forming in the first few hundred metres of the NBL. The upper region of the NBL is therefore separated from the surface and is less affected by surface emissions, which can act to destroy NO_3.

1.3 Measurements of NO_3 and N_2O_5

Following the first detection of NO_3 in the troposphere by DOAS (Platt et al., 1980) a wide range of surface-based field studies have sought to investigate the role of NO_3 in polluted and clean air environments (e.g., Smith et al., 1995; Allan et al., 2000; Geyer et al., 2001). These studies were generally focused on NO_3 only, as N_2O_5 does not absorb at visible wavelengths, rendering it undetectable using the DOAS technique. In order to overcome this limitation, a number of NO_3 instruments have recently been developed to infer N_2O_5 concentrations through the thermal manipulation of the equilibrium between NO_3 and N_2O_5. These experiments have generally used high-finesse cavity techniques (e.g., Dube et al., 2006; Brown et al., 2007a) or Laser Induced Fluorescence (LIF) (Matsumoto et al., 2005b) as in-situ detectors for the NO_3 produced from thermal dissociation of N_2O_5. Mixing ratios of up to 800 pptv of N_2O_5 were recently observed in Tokyo, Japan using one such technique (Matsumoto et al.,

2005a).

As the importance of NO_3 and N_2O_5 aloft has become apparent, a number of studies have sought to make vertically resolved measurements of NO_3 and N_2O_5 and this remains a very active area of interest (Aliwell and Jones, 1998; Fish et al., 1999; Geyer and Stutz, 2004; Stutz et al., 2004; Jones et al., 2005; Brown et al., 2007a). Brown et al. have recently reported airborne (2007a), tower (2007b), and ground based measurements (e.g. 2003b) in the USA, with more limited measurements being made by other groups over European regions (Aliwell and Jones, 1998; Povey et al., 1998; Penkett et al., 2007; McFiggans et al., 2010). Of particular note, there remain very few measurements at altitudes of 50–300 m a.g.l., where airborne measurements (Brown et al., 2005) have suggested peak concentrations may exist. Given the difficulties in performing measurements aloft in urban areas, fewer still data exist on NO_3 and N_2O_5 concentrations above densely populated areas.

To this end, this paper presents in-situ, high time resolution measurements of $[NO_3+N_2O_5]$ performed using LED-based broadband cavity enhanced absorption spectroscopy (LED-BBCEAS) over a month-long period at an altitude of 160 m over central London. These measurements formed part of the second phase of the Regent's Park and Tower Experiments (REPARTEE-II). We present an overview of the measurement dataset, together with an analysis of the lifetimes of NO_3 and N_2O_5 and the importance of these species to boundary layer chemistry in this region.

2 Experimental

2.1 The measurement site

The LED-BBCEAS instrument was deployed on level 35 of the British Telecommunications tower, 160 m a.g.l. in central London, UK (51° 31′ 17″ N 0° 08′ 20″ W) for 28 nights between 19 October 2007 and 15 November 2007. This tower site is relatively unusual in a cityscape in that it is taller, by a factor of approximately 9 (Barlow et al., 2009)

Discussion Paper | Discussion Paper | Discussion Paper | Discussion Paper

ACPD

10, 14347–14386, 2010

Night-time chemistry above London

A. K. Benton et al.

Title Page

Abstract | Introduction

Conclusions | References

Tables | Figures

◄ | ►|

◄ | ►

Back | Close

Full Screen / Esc

Printer-friendly Version

Interactive Discussion

than any other building within ~1 km of it. This leads to minimal local turbulence effects and loss of reactive atmospheric species to surfaces in the sampling vicinity. The tower is located close to large pollution sources, for example, Marylebone Road which is one of the busiest dual carriageways in London is approximately 300 m away from the foot of the tower. In contrast, the tower is also close (~700 m) to Regent's Park, where local air quality conditions are thought to be representative of urban background levels. Various chemical, particulate and meteorological measurements were made during REPARTEE-II and the reader is directed to Harrison et al. (2010) for further information.

2.2   Measurement technique: LED-BBCEAS

Broadband cavity enhanced absorption spectroscopy (BBCEAS) employing light emitting diode (LED) sources was used to provide in-situ measurements of the sum of NO_3 and N_2O_5 on the BT tower. The BBCEAS technique was introduced in 2003 by Fiedler et al. (2003) and has since been developed by a number of groups (Ruth et al., 2007; Washenfelder et al., 2008; Platt et al., 2009) including the current authors (Ball et al., 2004; Langridge et al., 2006, 2008a,b, 2009). A detailed description of the BBCEAS technique and the instrument used in this study is provided in Langridge et al. (2008a) and only a brief outline is provided here.

A BBCEAS measurement is conducted by exciting a high finesse optical cavity with a broadband continuous-wave light source. The intensity transmitted through the cavity rapidly establishes a steady state level, determined principally by the input optical power, the cavity mirror reflectivity and the absorption and scattering properties of the intra-cavity medium. By performing spectrally resolved measurements of the transmitted cavity intensity both in the absence (I_0) and presence (I) of the absorbing gas of interest, the sample absorption coefficient can be determined from Eq. (1) (Fiedler

et al., 2003).

$$Abs(\lambda) = \left(\frac{I_0(\lambda)}{I(\lambda)} - 1 \right) \frac{1 - R(\lambda)}{d_{\text{eff}}} \qquad (1)$$

where $R(\lambda)$ is the wavelength dependent reflectivity of the mirrors used to form the cavity and d_{eff} is the effective distance between cavity mirrors, accounting for differences between the true mirror-to-mirror distance and the length over which the sample gas fills the cavity.

BBCEAS provides a direct and highly sensitive means with which to determine unambiguously the concentration of an absorbing gas in-situ. High sensitivity arises as a direct result of confining the sample gas within a high finesse optical cavity, which essentially acts as an extremely effective multi-pass optical cell. By constructing the cavity with mirrors of appropriately high reflectivity (e.g. $R > 99.95\%$), optical path lengths of many kilometers can be achieved within a cell with a physical footprint of only approximately $1\,\text{m}^2$. This leads to sensitivities that are routinely better than $5 \times 10^{-9}\,\text{cm}^{-1}$ in 10 s (Langridge et al., 2008a). The ability of BBCEAS to determine absorber concentrations unambiguously, regardless of the presence of additional overlapping absorption features, results from the use of a broadband light source and wavelength resolved detection. Wavelength resolved spectra are captured upon every acquisition, allowing multivariate spectral fitting techniques, akin to those commonly used for differential optical absorption spectroscopy (DOAS) (Platt et al., 1980) to be used to separate contributions from molecular absorption/scattering and particulate scattering from the total extinction signal (Ball et al., 2004; Langridge et al., 2006; Ball and Jones, 2009).

One factor complicating the application of DOAS fitting principles to the analysis of BBCEAS spectra can be departure from Beer-Lambert absorption behaviour caused by strong narrow-band absorption structure, which remains unresolved by the BBCEAS measurements limited spectral resolution. This complication is important for the analysis of BBCEAS spectra of NO_3 absorption around 662 nm (used in this work), which overlaps with strong water vapour absorption in the $4\nu + \delta$ polyad. The treatment of

such complications has been described in detail by Langridge et al. (e.g. 2008a) and was applied here to analyse all ambient spectra.

2.3   LED-BBCEAS instrument

In the current work the BBCEAS instrument was operated across a wavelength range spanning 631–670 nm. This region captured the strong absorption peak of NO_3 centered at 662 nm corresponding to its B^2E'-X^2A_2 electronic transition, together with a significant portion of overlapping water vapour absorption structure. The instrument setup was very similar to that detailed in Langridge et al. (2008a), although operated with a slightly longer cavity length of 118.5 cm. The most important developments in this work were the use of a heated inlet to quantitatively convert ambient N_2O_5 to NO_3 and a heated cell to maintain the equilibrium in favour of NO_3.

The inlet was constructed from PFA tubing (Adtech ltd.) which has been shown to cause less NO_3 wall loss than alternative materials such as PTFE (Dube et al., 2006). Four individual lengths of 0.25″ OD, 0.125″ ID PFA tubing, each 50 cm long, were wrapped in heating tape and common insulation to form the inlet. The sample cell was constructed using 2 cm ID PFA tubing, which was also wrapped in heating tape and insulated. The inlet was joined to the sample cell at a 90° angle via a small machined PFA block employing push-fit o-ring seals. Both the inlet and sample cell were maintained at a temperature of 100 °C. A rotary pump and mass-flow controllers were used to pull air through the system at a constant flow rate of 6.8 SLPM (standard litres per minute). Assuming plug flow, residence times were 0.1 and 2.5 s in the inlet and cell, respectively. The residence time in the inlet was shown to be sufficient for >95% dissociation of N_2O_5 to NO_3 over the range conditions experienced during this deployment.

The cavity was mounted on an optical rail standing 1.4 m from the floor level (Fig. 2). The inlet was pointed towards the south-west (220°) and extended approximately 20 cm beyond a set of railings that enclosed the tower balcony.

2.4 Instrument operation

Spectra were collected using an integration time of 15 s for the duration of the project. Background spectra (I_0 in Eq. 1) were obtained by flushing the cavity with dry nitrogen at the same flow rate as used for ambient sampling. Since ambient (I) measurements were carried out in air, a correction was applied to the derived absorption coefficient to account for the small difference in Rayleigh scattering between N_2 and air. Collection of I_0 spectra was not fully automated during this deployment and the frequency with which they were acquired was determined, in large part, by the availability of access to the BT tower building. The intervals between I_0 spectra ranged from as short as 30 min to periods of several days, a typical deterioration in reflectivity over a period of 48 h was from a peak R (at λ=660 nm) of 0.9999 to 0.9995.

As shown in Eq. (1), the mirror reflectivity, $R(\lambda)$, is required to determine absolute absorber concentrations from BBCEAS measurements. This quantity can change over time, for example due to dirtying of the cavity mirrors or slight changes in optical alignment caused by temperature fluctuations. $R(\lambda)$ was measured periodically using phase shift cavity ringdown spectroscopy, as described by Langridge et al. (2008a). The mirror reflectivity was measured following every cavity re-alignment, mirror clean, or daily – whichever occurred most frequently, barring periods when access to the instrument wasn't possible for operational reasons. Calibrations of mirror reflectivity required approximately 1 h to complete and were thus carried out during daylight hours where possible. This minimised loss of data during the night, where [NO_3+N_2O_5] was most likely to be above the instrumental limit of detection (LOD).

Typically, the effective ringdown time (τ) at 660 nm of the nitrogen-flushed cavity was 25±1 μs, corresponding to a reflectivity $R(\lambda)$ of 0.9999±0.0001. Figure 3 shows a set of typical spectra measured during the course of the campaign. Both the NO_3 absorption structure together with that due to water vapour are clearly visible. NO_3 mixing ratios were retrieved by differential fitting and for these examples ranged from 33 to 298 pptv.

2.5 Uncertainty

LED-BBCEAS measurements are subject to both statistical errors, caused by uncertainty in the retrieval of spectral parameters, and systematic errors. The magnitudes of these errors are discussed here.

Statistical errors: the uncertainty in NO_3 spectral retrievals was found by determining the error in the gradient of a linear fit (Higbie, 1978) of the spectrally isolated NO_3 absorption component versus the NO_3 absorption cross section (Orphal et al., 2003). This method provides a good estimate for the measurement's LOD (Langridge, 2008). The magnitude of this uncertainty was around 2 pptv for $NO_3+N_2O_5$ for the vast majority of the campaign, but did rise for some periods to levels around 8 pptv, as shown in Fig. 4. Errors in the caused by changes in atmospheric pressure and uncertainties in the absorption cross section all contribute to this LOD. These increased LODs showed some correlation with periods of high aerosol extinction, which acted to limit the effective optical path length within the cavity and thus lead to poorer measurement signal-to-noise ratios, and on other occasions appeared to correlate with drifts in LED temperature which are known to affect its emission spectrum (Lee et al., 2010).

Systematic errors: the major uncertainty in the current measurements resulted from losses of reactive species to the walls of the inlet and sample cell. N_2O_5 wall losses are generally small, but those of NO_3 are significantly larger (Fuchs et al., 2008). Although ambient NO_3 generally accounted for a small part of the overall $NO_3+N_2O_5$ fraction in these studies, since almost all N_2O_5 is converted to NO_3 in the inlet of the instrument, it is important to consider the NO_3 transmission efficiency through the full system. Model calculations based on those by Bitter et al. (2005) and Fuchs et al. (2008) were used to deduce the instrument's transmission efficiency (TE) for $NO_3+N_2O_5$, taking into account the slightly different dimensions, flow rate and sample dilution in our inlet and cell. The first order wall loss rate for NO_3 on PFA reported by Dube et al. (2006) of $0.2 \pm 0.05 \, s^{-1}$ was used. The total net TE was found to be $68 \pm 8\%$.

2.6 Co-measurements

NO$_x$ measurements were carried out using a commercial NO$_x$ analyser (Thermo TE42C-TL), employing a heated Mo catalyst for conversion of NO$_2$ to NO, with a temporal resolution of 1 min. A UV absorption O$_3$ monitor (2B-Tech Dual Beam) was also
5 deployed (temporal resolution of 5 min), both at level T35 of the tower. Two measurements of turbulence in the vertical direction were used in this work: one from the 195 m level (mid-point of a 30 m vertical bin) of the suite of pulsed Doppler lidar (HALO Photonics, Pearson et al., 2009) measurements; and one from an ultrasonic anemometer (SA) (R3-50, Gill Instruments, UK) (Barlow et al., 2010; Wood et al., 2010) situated
10 at a height of 190 m on the top of the BT tower. A thorough discussion of vertical turbulence measurements during REPARTEE-II is detailed in Barlow et al. (2010). Furthermore, a measure of aerosol surface area (S_A) was derived using tandem (merged) Scanning Mobility Particle Sizer (SMPS) and Aerodynamic Particle Sizer (APS) measurements from level T35 of the tower (e.g., Shen et al., 2002; Dall'Osto et al., 2009).
15 The reader is directed to the summary paper for this campaign for further information (Harrison et al., 2010).

3 Results

LED-BBCEAS measurements commenced on 19 October 2007 at 10:00 UTC and concluded at 09:00 UTC on 15 November 2007. The full 15 s temporal resolution dataset
20 is shown in Fig. 4. Some spectra have been discarded due to significant misalignment of the cavity or very large increase in the retrieved LOD (a LOD value is reported for all times where analysis has been carried out but only data where NO$_3$+N$_2$O$_5$>LOD is shown in Fig. 4). Table 1 provides a statistical analysis of the raw dataset for periods when sufficient data exist to make it meaningful. As expected, a significant diurnal
25 trend is depicted as NO$_3$ is photolysed rapidly during the day and only rose above the LOD after, or within 30 min prior to sunset. A nocturnal (sunset to sunrise) mean

$NO_3+N_2O_5$ mixing ratio of 40 pptv was observed, with the highest mean of 166 pptv on the night of 30–31 October 2007.

There is high variability in the temporal structure and magnitude of the observed night-time enhancements of NO_3 and N_2O_5 during this campaign. Although there were no concurrent ground-level NO_3 or N_2O_5 measurements, mixing ratios of $NO_3+N_2O_5$ measured at ground level tend to be of the order of 10 pptv (McFiggans et al., 2010), supporting the notion of a significant vertical gradient in the NBL of these species. It is generally observed in this dataset (see Figs. 5 and 7) that any plume or injection of NO into the surrounding air corresponded to a very rapid extinction of NO_3 and N_2O_5, suggesting that NO_3 and N_2O_5 mixing ratios are highly dependent on their source strength and therefore the titration of NO against O_3. This is discussed further by examination of a case study period in Sect. 3.1.

3.1 Case study period: 30 October–1 November 2007

Figure 5 shows a detailed time series covering different chemical regimes of interest of $NO_3+N_2O_5$, O_3, (top panel) and NO, NO_2 (middle panel). The lower panel of Fig. 5 depicts two measurements of the variance of the vertical wind speed, σ_w^2 (m^2 s^2) which is a measure of vertical turbulence and hence, an indicator of the stability of the boundary layer. Under stable conditions, vertical turbulence will be reduced, whereas under unstable conditions turbulence is higher, such as during the daytime when warming of the surface causes convection.

The first night depicted (30–31 October) illustrates a strong anti correlation of $NO_3+N_2O_5$ with NO and a positive correlation with O_3. However, this correlation breaks down at approximately 04:30 UTC on 31 October, when O_3 mixing ratios remain moderately high (approximately 10 ppb), but there is a sudden apparent extinction of $NO_3+N_2O_5$. Of additional interest are the periods when the instrument was performing well but NO_3 and N_2O_5 levels were near or below this LOD. On some occasions, this appears to be due to a reduced NO_3 source as NO has titrated all available O_3 (for example sunset until 22:00 LT on 31 October). On other occasions, (for example

Night-time chemistry above London

A. K. Benton et al.

Title Page

Abstract | Introduction

Conclusions | References

Tables | Figures

◀ | ▶

◀ | ▶

Back | Close

Full Screen / Esc

Printer-friendly Version

Interactive Discussion

~02:00–~06:00 LT on 1 November,) O_3 and NO_2 are both present, and therefore the NO_3 source remains high, yet very low mixing ratios of $NO_3+N_2O_5$ are observed. In this period, the higher turbulence observed may contribute to lower $NO_3+N_2O_5$ through reduced mixing time or an increase in the rate of heterogeneous loss processes. It is noted that the increase in turbulence is accompanied by an uplift in NO and therefore an increase in NO at the tower height. However, in this instance this is not accompanied by a significant decrease in O_3 and is not thought to therefore directly affect NO_3 production. The small increase in σ_w^2 prior to sunrise (approximately indicated by the 2nd blue square from the left in the top panel of Fig. 5), supports the hypothesis that under conditions of low turbulence, mixing ratios of $NO_3+N_2O_5$ are likely to be greater as there is less potential for deposition.

3.2 Partitioning of the NO_3 and N_2O_5 equilibrium

Where NO_2 and temperature data was available, the measured $NO_3+N_2O_5$ was partitioned into NO_3 and N_2O_5 assuming equilibrium conditions. The equilibrium partitioning of NO_3 and N_2O_5 can be calculated from the known (temperature dependent) equilibrium constant for reaction (R3), provided, as is the case here, $[NO_2]$ (where a chemical species in square brackets is the number density concentration of that species) and temperature are known.

$$\frac{[NO_3]}{[N_2O_5]} = \frac{1}{K_{eq}(T)[NO_2]} \tag{2}$$

The justification for assuming that N_2O_5 is in equilibrium with NO_3 and NO_2. This was tested by a calculation of the time for a chemical system to relax to equilibrium (τ_{eq}), (e.g., Crowley et al., 2010).

$$\tau_{eq} = \frac{1}{k_{R3}[NO_2] + k_{R3}} \tag{3}$$

τ_{eq} was derived for the measurements described here, using the forward and reverse rate coefficients for (R3) from Sander et al. (2003) calculated for the range of encountered temperatures, together with measured NO_2 concentrations, to give a mean time to reach equilibrium of 2.34±1.66 s. The time to reach equilibrium was never more than 1 min, justifying the use of Eq. (2), as the median time for street-level emissions to reach tower height was calculated to be approximately 50 min (Barlow et al., 2010).

The mean equilibrium constant, $K_{eq}(T)$ (Sander, 2003), derived for the ambient temperature conditions of this campaign was $3.2\pm1.2\times10^{-10}$ cm^3 molecule^{-1} (Maximum: $K_{eq}(285\,K)$: 8.72×10^{-10} cm^3 molecule^{-1}, Maximum: $K_{eq}(277\,K)$: 1.79×10^{-10} cm^3 molecule^{-1}), giving a mean N_2O_5/NO_3 ratio over the campaign of 80. The NO_x analyser is likely to retrieve some fraction of NO_3 and N_2O_5 as NO_2, but as value of $[NO_3+N_2O_5]/[NO_x]$ was found to be less than 1% for the duration of the campaign no correction was applied.

Where NO_2 and temperature data was available, the $[NO_3+N_2O_5]$ was partitioned into NO_3 and N_2O_5. The high NO_2 levels shift the equilibrium in reaction (R3) so that almost all is N_2O_5, the maximum NO_3 observed at 31 October 2007 at 03:01 LT being 15±0.3 pptv with corresponding N_2O_5 at this point being around 499±1.63 pptv, (NO_2=4.3 ppbv, O_3∼7–8 ppbv).

The NO_2 mixing ratios for REPARTEE-II were moderately high compared with other urban measurements (WHO, 2006) nocturnal mean ∼20 ppbv (see Fig. 7), although not unusual for a central London site. The emissions profile and ambient temperatures of around 3–10 °C in UK Autumn, lead to a high dominance of N_2O_5 in reaction (3). The fraction of $[NO_3]/[N_2O_5]$ was as low as 1–4% throughout the campaign with a mean of 2%. Therefore, where NO_2 data is unavailable and thus the equilibrium partitioning of NO_3 and N_2O_5 cannot be determined, it is reasonable to make the assumption that $[NO_3+N_2O_5]\approx[N_2O_5]$.

A useful parameter to identify, when dealing with a suite of NO_x measurements, is the fraction of NO_x that is stored in the nocturnal equilibrium between NO_3 and N_2O_5 (R3): $F(NO_x)$ given by Brown et al. (2004) and McLaren et al. (2004). Smaller values

of $F(NO_x)$ can be indicative of shorter lifetimes; shorter lifetimes suggest rapid sinks for N_2O_5.

$$F(NO_x) = \frac{[NO_3] + 2[N_2O_5]}{[NO_2] + [NO_3] + 2[N_2O_5]} \tag{4}$$

A median value of $F(NO_x)$ for REPARTEE-II night-times is around 0.05 with a mean of
5 only 1% (Fig. 10). This is somewhat lower than previous studies in moderately polluted MBL and aloft ($\sim$0.05–0.2), (Brown et al., 2004; McLaren et al., 2010). Elevated mixing ratios of NO_2 also act to decrease $F(NO_x)$.

3.3 Correlations with ancillary data

No apparent correlation of [NO_3+N_2O_5] with wind direction was observed (Fig. 6), nor
10 with air mass history from 5-day back trajectory calculations (Rolph, 2003), (Table 1) consistent with the measurement site being unbiased in terms of direction of local emissions of NO_x. The probability distribution of wind directionality in Fig. 6 depicts that this was a common directional wind sector during REPARTEE-II, but only mixing ratios of <100 pptv for NO_3+N_2O_5 were measured at these times.
15 Figure 7 shows a summary of BBCEAS-derived components of the campaign dataset, along with some useful ancillary parameters for comparison. The maximum retrieved partitioned mixing ratios for the campaign for 1 h averages were 500 pptv for N_2O_5 and 10 pptv for NO_3. A negative correlation of night-time NO_3+N_2O_5 with NO (strong) and NO_2 (weak) and a positive correlation with O_3 are depicted in Fig. 8. The
20 negative correlation with NO_2 is likely to be a result of an increased NO source for NO_2 production coinciding with a decrease in NO_3, as high periods of NO will act to decrease NO_3 and increase NO_2.

Turbulence measurements were used to indicate the meteorological regimes encountered in the NBL. The lidar is expected to slightly underestimate the vertical veloc-
25 ity variance slightly compared to the sonic anemometer under more stable conditions due to the differing sampling rate (4 s compared to 20 Hz, respectively), this divergence

is more apparent in Fig. 7. Figure 9 shows that [NO$_3$+N$_2$O$_5$] is proportional to the inverse of both the mean night-time and maximum night-time σ_w^2. This supports the theory of night-time [NO$_3$+N$_2$O$_5$] enhancements occurring when conditions are stable, turbulence is suppressed, and the BT tower measurements are somewhat decoupled from emissions from the surface.

3.4 Calculated lifetimes of NO$_3$ and N$_2$O$_5$

The lifetimes of NO$_3$, (τ(NO$_3$)) and N$_2$O$_5$, (τ(N$_2$O$_5$)) are useful for determining the magnitude of sources and sinks of NO$_y$ in a particular regime. The derivations shown in Eqs. (5) and (6) rely on the assumption of a steady state for the production and loss of NO$_3$ and N$_2$O$_5$ and have been used in many studies to derived useful parameters regarding night-time NO$_y$

$$\tau(\text{NO}_3) = \frac{[\text{NO}_3]}{k_2 \left[\text{O}_3\right] \left[\text{NO}_2\right]} \tag{5}$$

$$\tau(\text{N}_2\text{O}_5) = \frac{[\text{N}_2\text{O}_5]}{k_2 \left[\text{O}_3\right] \left[\text{NO}_2\right]} \tag{6}$$

It has been shown (Brown et al., 2003a) that for conditions such as those during REPARTEE-II, where moderate to high NO$_2$ (mean night-time NO$_2 \sim 20$ ppbv) and low temperatures are experienced, that although NO$_3$ and N$_2$O$_5$ are very likely to be in equilibrium (see Sect. 3.2), the time for reaching a steady state for NO$_3$ and/or N$_2$O$_5$ is likely to be several hours. This assumption was tested using a simple box model (not shown) and indeed, the derivatives of the NO$_3$ and N$_2$O$_5$ mixing ratios were found to confirm that a steady state is unlikely to be established over the period of one night. In addition, a measurement over such a small volume such as that by LED-BBCEAS diverges from steady state through transport and turbulence, as well as chemical effects. Therefore, a steady state approximation was considered unlikely to be appropriate for

much of this study. It was therefore deemed prudent to compare calculations of both a steady state lifetime and a lifetime for NO_3 and N_2O_5 taking into account the likely absence of a steady state (τ^*) as per Eq. (7) (McLaren, 2009).

$$\tau^*(N_2O_5 \text{ or } NO_3) = \frac{[N_2O_5 \text{ or } NO_3]}{k_2[O_3][NO_2] - \frac{d[NO_3]}{dt} - \frac{d[N_2O_5]}{dt}} \qquad (7)$$

5 The differential of NO_3 and N_2O_5 with respect to time was calculated using a 3 point average of 15 s data. The result of this calculation was insensitive to using larger moving averages as the measured mixing ratios were highly variable on many temporal scales. It is noted that both lifetime analyses neglect any influence of transport effects. Both determinations of ss via Eqs. (5) and (6); and τ^* using Eq. (7) (for both NO_3

10 and N_2O_5) have been performed here, and in contrast to the only previous reported example of this comparison (McLaren et al., 2010), a significant difference in the results of the two methods of lifetime calculation are reported here, with the latter resulting in highly variable lifetimes, with a mean value lower by approximately 75% of its steady state counterpart. This can be seen by the diurnal trends in Fig. 10. Of particular note

15 is that the mean lies above the 95th percentile for much of the τ^* (non-steady state), particularly in the second half of the night, showing the highly variable nature of τ^*.

3.5 Aerosol uptake of N_2O_5

The inability to assume a steady state in under the [NO_2] and typical UK autumnal temperature conditions of REPARTEE-II renders the determination of the N_2O_5 uptake

20 coefficient, $\gamma(N_2O_5)$, difficult as many widely used determinations of k_{het} require the assumption of a steady state between NO_3 and N_2O_5. The rate of uptake for reaction (R4), k_{het}, was derived from Eq. (8) (Riemer et al., 2003):

$$k_{het} = \frac{1}{4}c_{N_2O_5}S_A\gamma(N_2O_5) \qquad (8)$$

Here, $c_{N_2O_5}$ is the mean molecular velocity of N_2O_5 and S_A is the integrated surface

25 area for all particles of <1 μm diameter, (see Sect. 2.6) which takes into account the

diffusion limitations to particles (Bertram and Thornton, 2009). S_A ranged from 200–1000 $\mu m^2\, cm^{-2}$. The uptake coefficient, $\gamma(N_2O_5)$, was derived from a parameterisation detailed in Riemer et al. (2003) as a function of relative humidity (RH) and the ratio of mass fractions of sulphate and nitrate in aerosols (Nemitz et al., 2010). Both the mass fraction and S_A (Fig. 11) were highly variable during the campaign. Figure 11 shows a time series of calculated k_{het} (Fig. 11), along with measured S_A and calculated $\gamma(N_2O_5)$. Mean k_{het} from these measurements was $0.17\pm0.08\, min^{-1}$.

The short lifetimes depicted suggest rapid conversion to HNO_3 via reaction (R4). Reaction of N_2O_5 with H_2O on aerosol surfaces is considered to be the principal night-time pathway for HNO_3 formation, although there is likely to be some contribution from the reaction of NO_3 with anthropogenic VOCs (such as alkenes). Assuming that each NO_3 radical goes onto form N_2O_5 and then hydrolyses to two HNO_3 molecules, the contribution to $[HNO_3]$ from reaction (R4) can be calculated via two methods (Wood et al., 2005).

$$[HNO_3] = 2\int \frac{[N_2O_5]}{\tau_{ss}(N_2O_5)}dt \approx 2\int k_2[NO_2][O_3]dt \tag{9}$$

The total integrated mixing ratio of HNO_3 was calculated for each night (sunset to sunrise) by both methods for complete nights where required ancillary datasets exist, (see Table 2) and was found to range from 2.4–11.3 ppbv via calculation using BBCEAS-inferred N_2O_5 mixing ratios and by 6.6–13.5 ppbv using NO_2 and O_3 mixing ratios as measured during the campaign with the latter an average of 2 ppbv per night greater than the former. This difference could be due to the large calculated error in the transmission efficiency of the BBCEAS inlet potentially leading to underestimations in $[N_2O_5]$, or due to the approximations made in assuming a steady state for calculation of $\tau_{ss}(N_2O_5)$, or losses other than to HNO_3 may be present, such as those by NO_3, or a combination of both factors. It should also be considered that reaction of HNO_3 with ammonia or sea salt would yield a significant aerosol concentration. Using one of the case study nights of 30–31 October, $[HNO_3]$ was calculated to be 7.0 ± 1.5 ppbv using

mixing ratios of N_2O_5 and its calculated steady-state lifetime, and 8.6±0.26 ppbv using NO_2 and O_3 mixing ratios which accounts for approximately 22 µg m^{-3} HNO_3 as an integrated total for this night. As HNO_3 mixing ratio measurements averaged approximately 0.17 ppbv during this night (Nemitz et al., 2010), this represents a very small fraction of the total integrated mixing ratio for that night of the order of 0.001%.

4 Summary and conclusions

In this paper we have demonstrated the first sustained deployment of LED-BBCEAS technique in a month-long field campaign. To our knowledge these are the first measurements of NO_3 and N_2O_5 above a developed megacity and give an in-situ insight into the complexity of urban nocturnal boundary layer chemistry in such a region. The instrument demonstrated the ability to measure make continuous sensitive measurements over periods long enough to perform quantitative diurnal trend analyses and produced an urban dataset useful for those wishing to test models on urban areas. A large variation in night-time concentrations was observed, with some high N_2O_5 (<800 pptv) concentrations measured. N_2O_5 appears to be very reactive and calculated lifetimes were short. In addition to nights where large enhancements are observed, there were nights when the BBCEAS instrument was performing well and concentrations of N_2O_5 were below the LOD of around 2 pptv. These nights are of additional interest as they suggest an extremely large sink to source ratio, which appears to be unaccounted for by observed aerosol components. The complexity of the data rendered typical steady state analysis difficult and demonstrate the challenge of interpreting in-situ observations of moderate lifetime species in a highly heterogeneous environment. The equilibrium between NO_3 and N_2O_5 was calculated from NO_2 and ambient temperature to be weighted heavily in favour of N_2O_5 and the maximum mixing ratio of NO_3 was 10 pptv over 1 h. Correlation between the magnitude of [NO_3+N_2O_5] and [O_3] was observed along with a strong negative correlation with [NO] but it does not appear to be a simple function. A combination of chemical and physical sources and sinks appear to be

important in determining [NO$_3$] and [N$_2$O$_5$], a theory supported by the negative correlation with a proxy for night-time turbulence. The short NO$_3$ and N$_2$O$_5$ lifetimes and high NO$_2$ conditions depict a low value of F(NO$_x$). However, this does not necessarily mean night-time nitrate chemistry is negligible, rather that the sinks for N$_2$O$_5$ may be very rapid, leading to a potential source of nitrate in aerosols. Departures from the NO$_3$ N$_2$O$_5$ equilibrium do not appear to be significant, though the high NO$_2$ and low temperatures slow the systems approach to a steady-state. A comparison between steady state and non-steady state analyses of the lifetimes of N$_2$O$_5$ and NO$_3$ was performed and it was found that the system was unlikely to be in steady state, rendering steady state analysis of heterogeneous loss of N$_2$O$_5$ difficult. Estimates of the heterogeneous uptake of N$_2$O$_5$ suggest a small contribution of around 8 ppbv per night of HNO$_3$ via this route and depicting a potential pathway for other significant losses of NO$_3$ or N$_2$O$_5$. These results demonstrate the complexity of small scale NBL chemical processes and how they may contribute to NO$_y$ loss budgets.

References

Aliwell, S. R. and Jones, R. L.: Measurements of tropospheric NO$_3$ at midlatitude, J. Geophys. Res.-Atmos., 103, 5719–5727, 1998.

Allan, B. J., McFiggans, G., Plane, J. M. C., Coe, H., and McFadyen, G. G.: The nitrate radical in the remote marine boundary layer, J. Geophys. Res.-Atmos., 105, 24191–24204, 2000.

Atkinson, R.: Atmospheric chemistry of VOCs and NO_x, Atmos. Environ., 34, 2063–2101, 2000.

Ball, S. and Jones, R.: Broadband cavity ring-down spectroscopy, in: Cavity Ring-Down Spectroscopy: Techniques and Applications, edited by: Berden, G. and Engeln, R., Wiley-Blackwell, Oxford, xix, 57–87, 2009.

Ball, S. M., Langridge, J. M., and Jones, R. L.: Broadband cavity enhanced absorption spectroscopy using light emitting diodes, Chem. Phys. Lett., 398, 68–74, 2004.

Barlow, J. F., Dobre, A., Smalley, R. J., Arnold, S. J., Tomlin, A. S., and Belcher, S. E.: Referencing of street-level flows measured during the DAPPLE 2004 campaign, Atmos. Environ., 43, 5536–5544, doi:10.1016/j.atmosenv.2009.05.021, 2009.

Bertram, T. H. and Thornton, J. A.: Toward a general parameterization of N2O5 reactivity on aqueous particles: the competing effects of particle liquid water, nitrate and chloride, Atmos. Chem. Phys., 9, 8351–8363, doi:10.5194/acp-9-8351-2009, 2009.

Bitter, M., Ball, S. M., Povey, I. M., and Jones, R. L.: A broadband cavity ringdown spectrometer for in-situ measurements of atmospheric trace gases, Atmos. Chem. Phys., 5, 2547–2560, doi:10.5194/acp-5-2547-2005, 2005.

Brown, S. S.: Absorption spectroscopy in high-finesse cavities for atmospheric studies, Chem. Rev., 103, 5219–5238, doi:10.1021/cr020645c, 2003.

Brown, S. S., Stark, H., and Ravishankara, A. R.: Applicability of the steady state approximation to the interpretation of atmospheric observations of NO_3 and N_2O_5, J. Geophys. Res.-Atmos., 108(D17), 4539, doi:10.1029/2003JD003407, 2003a.

Brown, S. S., Stark, H., Ryerson, T. B., Williams, E. J., Nicks, D. K., Trainer, M., Fehsenfeld, F. C., and Ravishankara, A. R.: Nitrogen oxides in the nocturnal boundary layer: simultaneous in situ measurements of NO_3, N_2O_5, NO_2, NO, and O_3, J. Geophys. Res.-Atmos., 108(D9), 4299, doi:10.1029/2002JD002917, 2003b.

Brown, S. S., Dibb, J. E., Stark, H., Aldener, M., Vozella, M., Whitlow, S., Williams, E. J., Lerner, B. M., Jakoubek, R., Middlebrook, A. M., DeGouw, J. A., Warneke, C., Goldan, P. D., Kuster, W. C., Angevine, W. M., Sueper, D. T., Quinn, P. K., Bates, T. S., Meagher, J. F., Fehsenfeld, F. C., and Ravishankara, A. R.: Nighttime removal of NO_x in the summer marine boundary layer, Geophys. Res. Lett., 31(7), L07108, doi:10.1029/2004GL019412, 2004.

Brown, S. S., Osthoff, H. D., Stark, H., Dube, W. P., Ryerson, T. B., Warneke, C., de Gouw, J. A., Wollny, A. G., Parrish, D. D., Fehsenfeld, F. C., and Ravishankara, A. R.: Aircraft observations of daytime NO_3 and N_2O_5 and their implications for tropospheric chemistry, J. Photoch.

Night-time chemistry above London

A. K. Benton et al.

Title Page

Abstract	Introduction
Conclusions	References
Tables	Figures

◄ | ►|

◄ | ►

Back | Close

Full Screen / Esc

Printer-friendly Version

Interactive Discussion

Photobio. A., 176, 270–278, 2005.

Brown, S. S., Dube, W. P., Osthoff, H. D., Stutz, J., Ryerson, T. B., Wollny, A. G., Brock, C. A., Warneke, C., De Gouw, J. A., Atlas, E., Neuman, J. A., Holloway, J. S., Lerner, B. M., Williams, E. J., Kuster, W. C., Goldan, P. D., Angevine, W. M., Trainer, M., Fehsenfeld, F. C., and Ravishankara, A. R.: Vertical profiles in NO_3 and N_2O_5 measured from an aircraft: results from the NOAA P-3 and surface platforms during the New England Air Quality Study 2004, J. Geophys. Res.-Atmos., 112(D22), D22304, doi:10.1029/2007jd008883, 2007a.

Brown, S. S., Dubé, W. P., Osthoff, H. D., Wolfe, D. E., Angevine, W. M., and Ravishankara, A. R.: High resolution vertical distributions of NO_3 and N_2O_5 through the nocturnal boundary layer, Atmos. Chem. Phys., 7, 139–149, doi:10.5194/acp-7-139-2007, 2007b.

Crowley, J. N., Schuster, G., Pouvesle, N., Parchatka, U., Fischer, H., Bonn, B., Bingemer, H., and Lelieveld, J.: Nocturnal nitrogen oxides at a rural mountain-site in south-western Germany, Atmos. Chem. Phys., 10, 2795–2812, doi:10.5194/acp-10-2795-2010, 2010.

Dall'Osto, M., Harrison, R. M., Coe, H., Williams, P. I., and Allan, J. D.: Real time chemical characterization of local and regional nitrate aerosols, Atmos. Chem. Phys., 9, 3709–3720, doi:10.5194/acp-9-3709-2009, 2009.

Dentener, F. J. and Crutzen, P. J.: Reaction of N_2O_5 on tropospheric aerosols – impact on the global distributions of NO_x, O_3, and OH, J. Geophys. Res.-Atmos., 98, 7149–7163, 1993.

Dube, W. P., Brown, S. S., Osthoff, H. D., Nunley, M. R., Ciciora, S. J., Paris, M. W., McLaughlin, R. J., and Ravishankara, A. R.: Aircraft instrument for simultaneous, in situ measurement of NO_3 and N_2O_5 via pulsed cavity ring-down spectroscopy, Rev. Sci. Instrum., 77(3), 034101, doi:10.1063/1.2176058, 2006.

Fiedler, S. E., Hese, A., and Ruth, A. A.: Incoherent broad-band cavity-enhanced absorption spectroscopy, Chem. Phys. Lett., 371, 284–294, 2003.

Fish, D. J., Shallcross, D. E., and Jones, R. L.: The vertical distribution of NO_3 in the atmospheric boundary layer, Atmos. Environ., 33, 687–691, 1999.

Fuchs, H., Dube, W. P., Cicioira, S. J., and Brown, S. S.: Determination of inlet transmission and conversion efficiencies for in situ measurements of the nocturnal nitrogen oxides, NO_3, N_2O_5 and NO_2, via pulsed cavity ring-down spectroscopy, Anal. Chem., 80, 6010–6017, 2008.

Geyer, A., Alicke, B., Konrad, S., Schmitz, T., Stutz, J., and Platt, U.: Chemistry and oxidation capacity of the nitrate radical in the continental boundary layer near Berlin, J. Geophys. Res.-Atmos., 106, 8013–8025, 2001.

Geyer, A. and Stutz, J.: Vertical profiles of NO_3, N_2O_5, O_3, and NO_x in the nocturnal boundary

layer: 2. Model studies on the altitude dependence of composition and chemistry, J. Geophys. Res.-Atmos., 109(D16), D16399, doi:10.1029/2004jd005217, 2004.

Hallquist, M., Stewart, D. J., Baker, J., and Cox, R. A.: Hydrolysis of N_2O_5 on submicron sulfuric acid aerosols, J. Phys. Chem. A., 104, 3984–3990, 2000.

Hammer, P. D., Dlugokencky, E. J., and Howard, C. J.: Kinetics of the gas-phase reaction $NO+NO_3 \rightarrow 2NO_2$, J. Phys. Chem., 90, 2491–2496, 1986.

Higbie, J.: Uncertainty in a least-squares fit, Am. J. Phys., 46, 945–945, 1978.

Jones, R. L., Ball, S. M., and Shallcross, D. E.: Small scale structure in the atmosphere: implications for chemical composition and observational methods, Faraday. Discuss., 130, 165–179, doi:10.1039/b502633b, 2005.

Langridge, J. M., Ball, S. M., and Jones, R. L.: A compact broadband cavity enhanced absorption spectrometer for detection of atmospheric NO_2 using light emitting diodes, Analyst, 131, 916–922, doi:10.1039/b605636a, 2006.

Langridge, J. M.: Development and atmospheric applications of a novel broadband cavity enhanced absorption spectrometer, Dept. of Chem., Univ. of Cambridge, Cambridge, 2008.

Langridge, J. M., Ball, S. M., Shillings, A. J. L., and Jones, R. L.: A broadband absorption spectrometer using light emitting diodes for ultrasensitive, in situ trace gas detection, Rev. Sci. Instrum., 79(12), 123110, doi:10.1063/1.3046282, 2008a.

Langridge, J. M., Laurila, T., Watt, R. S., Jones, R. L., Kaminski, C. F., and Hult, J.: Cavity enhanced absorption spectroscopy of multiple trace gas species using a supercontinuum radiation source, Opt. Express., 16, 10178–10188, 2008b.

Langridge, J. M., Gustafsson, R. J., Griffiths, P. T., Cox, R. A., Lambert, R. M., and Jones, R. L.: Solar driven nitrous acid formation on building material surfaces containing titanium dioxide: a concern for air quality in urban areas?, Atmos. Environ., 43, 5128–5131, 2009.

Lee, J. D., McFiggans, G., Allan, J. D., Baker, A. R., Ball, S. M., Benton, A. K., Carpenter, L. J., Commane, R., Finley, B. D., Evans, M., Fuentes, E., Furneaux, K., Goddard, A., Good, N., Hamilton, J. F., Heard, D. E., Herrmann, H., Hollingsworth, A., Hopkins, J. R., Ingham, T., Irwin, M., Jones, C. E., Jones, R. L., Keene, W. C., Lawler, M. J., Lehmann, S., Lewis, A. C., Long, M. S., Mahajan, A., Methven, J., Moller, S. J., Mller, K., Mller, T., Niedermeier, N., O'Doherty, S., Oetjen, H., Plane, J. M. C., Pszenny, A. A. P., Read, K. A., Saiz-Lopez, A., Saltzman, E. S., Sander, R., von Glasow, R., Whalley, L., Wiedensohler, A., and Young, D.: Reactive Halogens in the Marine Boundary Layer (RHaMBLe): the tropical North Atlantic experiments, Atmos. Chem. Phys., 10, 1031–1055, doi:10.5194/acp-10-1031-2010, 2010.

Night-time chemistry above London

A. K. Benton et al.

Matsumoto, J., Imai, H., Kosugi, N., and Kaji, Y.: In situ measurement of N_2O_5 in the urban atmosphere by thermal decomposition/laser-induced fluorescence technique, Atmos. Environ., 39, 6802–6811, 2005a.

Matsumoto, J., Kosugi, N., Imai, H., and Kajii, Y.: Development of a measurement system for nitrate radical and dinitrogen pentoxide using a thermal conversion/laser-induced fluorescence technique, Rev. Sci. Instrum., 76(6), 064101, doi:10.1063/1.1927098, 2005b.

McFiggans, G., Bale, C. S. E., Ball, S. M., Beames, J. M., Bloss, W. J., Carpenter, L. J., Dorsey, J., Dunk, R., Flynn, M. J., Furneaux, K. L., Gallagher, M. W., Heard, D. E., Hollingsworth, A. M., Hornsby, K., Ingham, T., Jones, C. E., Jones, R. L., Kramer, L. J., Langridge, J. M., Leblanc, C., LeCrane, J.-P., Lee, J. D., Leigh, R. J., Longley, I., Mahajan, A. S., Monks, P. S., Oetjen, H., Orr-Ewing, A. J., Plane, J. M. C., Potin, P., Shillings, A. J. L., Thomas, F., von Glasow, R., Wada, R., Whalley, L. K., and Whitehead, J. D.: Iodine-mediated coastal particle formation: an overview of the Reactive Halogens in the Marine Boundary Layer (RHaMBLe) Roscoff coastal study, Atmos. Chem. Phys., 10, 2975–2999, doi:10.5194/acp-10-2975-2010, 2010.

McLaren, R., Salmon, R. A., Liggio, J., Hayden, K. L., Anlauf, K. G., and Leaitch, W. R.: Night-time chemistry at a rural site in the Lower Fraser Valley, Atmos. Environ., 38, 5837–5848, 2004.

McLaren, R., Wojtal, P., Majonis, D., McCourt, J., Halla, J. D., and Brook, J.: NO_3 radical measurements in a polluted marine environment: links to ozone formation, Atmos. Chem. Phys., 10, 4187–4206, doi:10.5194/acp-10-4187-2010, 2010.

Mentel, T. F., Bleilebens, D., and Wahner, A.: A study of nighttime nitrogen oxide oxidation in a large reaction chamber – the fate of NO_2, N_2O_5, HNO_3, and O_3 at different humidities, Atmos. Environ., 30, 4007–4020, 1996.

Orphal, J., Fellows, C. E., and Flaud, P. M.: The visible absorption spectrum of NO_3 measured by high-resolution Fourier transform spectroscopy, J. Geophys. Res.-Atmos., 108(D3), 4077, doi:10.1029/2002JD002489, 2003.

Pearson, G., Davies, F., and Collier, C.: An analysis of the performance of the UFAM pulsed doppler lidar for observing the boundary layer, J. Atmos. Ocean. Tech., 26, 240–250, 2009.

Penkett, S. A., Burgess, R. A., Coe, H., Coll, I., Hov, O., Lindskog, A., Schmidbauer, N., Solberg, S., Roemer, M., Thijsse, T., Beck, J., and Reeves, C. E.: Evidence for large average concentrations of the nitrate radical (NO_3) in Western Europe from the HANSA hydrocarbon database, Atmos. Environ., 41, 3465–3478, 2007.

Night-time chemistry above London

A. K. Benton et al.

Title Page

Abstract	Introduction
Conclusions	References
Tables	Figures

◄ | ►

◄ | ►

Back | Close

Full Screen / Esc

Printer-friendly Version

Interactive Discussion

Platt, U., Perner, D., Winer, A. M., Harris, G. W., and Pitts, J. N.: Detection of NO_3 in the polluted troposphere by differential optical-absorption, Geophys. Res. Lett., 7, 89–92, 1980.

Platt, U., Meinen, J., Pöhler, D., and Leisner, T.: Broadband Cavity Enhanced Differential Optical Absorption Spectroscopy (CE-DOAS) – applicability and corrections, Atmos. Meas. Tech., 2, 713–723, doi:10.5194/amt-2-713-2009, 2009.

Povey, I. M., South, A. M., de Roodenbeke, A. T., Hill, C., Freshwater, R. A., and Jones, R. L.: A broadband lidar for the measurement of tropospheric constituent profiles from the ground, J. Geophys. Res.-Atmos., 103, 3369–3380, 1998.

Riemer, N., Vogel, H., Vogel, B., Schell, B., Ackermann, I., Kessler, C., and Hass, H.: Impact of the heterogeneous hydrolysis of N_2O_5 on chemistry and nitrate aerosol formation in the lower troposphere under photosmog conditions, J. Geophys. Res.-Atmos, 108(D4), 4144, doi:10.1029/2002JD002436, 2003.

Ruth, A. A., Orphal, J., and Fiedler, S. E.: Fourier-transform cavity-enhanced absorption spectroscopy using an incoherent broadband light source, Appl. Optics., 46, 3611–3616, 2007.

Shen, S., Jaques, P. A., Zhu, Y. F., Geller, M. D., and Sioutas, C.: Evaluation of the SMPS-APS system as a continuous monitor for measuring $PM_{2.5}$, PM_{10} and coarse ($PM_{2.5-10}$) concentrations, Atmos. Environ., 36, 3939–3950, 2002.

Smith, N., Plane, J. M. C., Nien, C. F., and Solomon, P. A.: Nighttime radical chemistry in the San-Joaquin valley, Atmos. Environ., 29, 2887–2897, 1995.

Stark, H., Lerner, B. M., Schmitt, R., Jakoubek, R., Williams, E. J., Ryerson, T. B., Sueper, D. T., Parrish, D. D., and Fehsenfeld, F. C.: Atmospheric in situ measurement of nitrate radical (NO_3) and other photolysis rates using spectroradiometry and filter radiometry, J. Geophys. Res.-Atmos., 112(D10), D10S04, doi:10.1029/2006JD007578, 2007.

Stutz, J., Alicke, B., Ackermann, R., Geyer, A., White, A., and Williams, E.: Vertical profiles of NO_3, N_2O_5, O_3, and NO_x in the nocturnal boundary layer – Part 1. Observations during the Texas Air Quality Study 2000, J. Geophys. Res.-Atmos., 109(D16), D16398, doi:10.1029/2004jd005216, 2004.

Wangberg, I., Etzkorn, T., Barnes, I., Platt, U., and Becker, K. H.: Absolute determination of the temperature behavior of the $NO_2+NO_3+(M)\leftrightarrow N_2O_5+(M)$ equilibrium, J. Phys. Chem. A., 101, 9694–9698, 1997.

Washenfelder, R. A., Langford, A. O., Fuchs, H., and Brown, S. S.: Measurement of glyoxal using an incoherent broadband cavity enhanced absorption spectrometer, Atmos. Chem. Phys., 8, 7779–7793, doi:10.5194/acp-8-7779-2008, 2008.

WHO: Air Quality Guidelines: Global Update 2005: Particulate Matter, Ozone, Nitrogen Dioxide, and Sulfur Dioxide, World Health Organization, Copenhagen, ix, 484 pp., 2006.

Wood, E. C., Bertram, T. H., Wooldridge, P. J., and Cohen, R. C.: Measurements of N_2O_5, NO_2, and O_3 east of the San Francisco Bay, Atmos. Chem. Phys., 5, 483–491, doi:10.5194/acp-5-483-2005, 2005.

Night-time chemistry above London

A. K. Benton et al.

Table 1. Statistics for night-time measurements of $[NO_3+N_2O_5]$/pptv. Night-time as defined by sunrise/sunset times. N:dataset size; 75% and 95% refers to 75th and 95th percentile; All data <LOD replaced with the median of the variable detection limit of around 2 pptv and zero. Air masses grouped as indicated by a general inspection of 5-day back trajectories (Rolph, 2003) and coded by predominant origin as: P: Polar, EC: easterly continental; A: Altantic:, NC: northern continental.

Night	N	Min	25%	Median	Mean	75%	95%	Max	Air mass
19 Oct–20 Oct	4368	<LOD	<LOD	4	12	15	44	161	P
20 Oct–21 Oct	4214	<LOD	3	9	57	47	337	789	P
21 Oct–22 Oct	4093	<LOD	<LOD	<LOD	3	<LOD	11	85	NC
22 Oct–23 Oct	6872	<LOD	<LOD	11	23	29	93	390	EC
23 Oct–24 Oct	1946	<LOD	4	9	12	15	38	95	EC
24 Oct–25 Oct	2687	<LOD	<LOD	<LOD	<LOD	<LOD	<LOD	55	EC
25 Oct–26 Oct	4280	<LOD	<LOD	<LOD	<LOD	<LOD	<LOD	183	EC
29 Oct–30 Oct	207	<LOD	19	29	47	68	124	135	A
30 Oct–31 Oct	4540	<LOD	8	120	166	298	437	633	A
31 Oct–1 Nov	4307	<LOD	<LOD	<LOD	4	4	20	117	A
1 Nov–2 Nov	3977	<LOD	4	37	60	99	183	283	A
2 Nov–3 Nov	1206	<LOD	<LOD	<LOD	8	4	45	208	A
5 Nov–6 Nov	4633	<LOD	32	52	49	65	90	132	P
6 Nov–7 Nov	5131	<LOD	<LOD	12	31	45	123	237	A
7 Nov–8 Nov	4552	<LOD	9	25	32	46	92	182	A
9 Nov–10 Nov	5155	<LOD	22	43	48	70	106	197	A
10 Nov–11 Nov	5207	<LOD	14	25	28	40	59	119	A
12 Nov–13 Nov	4881	<LOD	<LOD	13	96	123	448	796	P
13 Nov–14 Nov	5260	<LOD	32	56	72	109	170	238	P
14 Nov–15 Nov	4924	<LOD	27	58	64	92	149	201	NC
All night-time data	82 453	<LOD	<LOD	16	44	52	180	796	

Table 2. Total calculated night-time [HNO$_3$], using [N$_2$O$_5$] and τ_{ss}(N$_2$O$_5$), (2nd column); and using k_2, [NO$_2$] and [O$_3$], (3rd column) of Eq. (9) for nights where a continuous dataset for all parameters were used.

Night	[HNO$_3$]$_a$/ppbv	[HNO$_3$]$_b$/ppbv
30 Oct–31 Oct	7.0±1.5	8.6±0.26
31 Oct–1 Nov	2.4±0.50	7.0±0.2
1 Nov–2 Nov	9.1±1.9	10.5±0.3
5 Nov–6 Nov	9.2±1.9	9.8±0.3
6 Nov–7 Nov	4.5±1.0	6.6±0.2
7 Nov–8 Nov	11.3±2.4	13.5±0.4
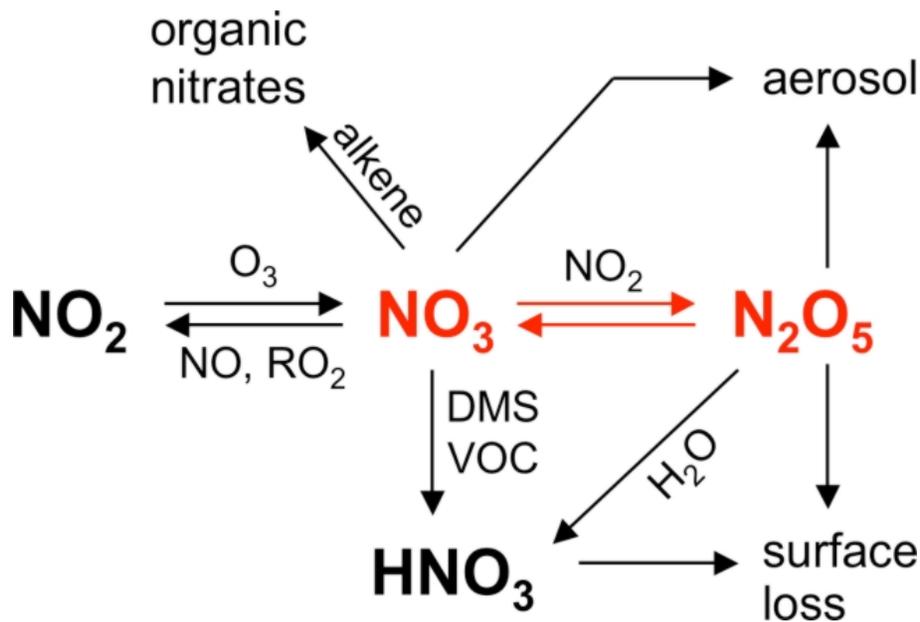
Fig. 1. Simplified schematic of nocturnal NO$_y$ chemical processes.
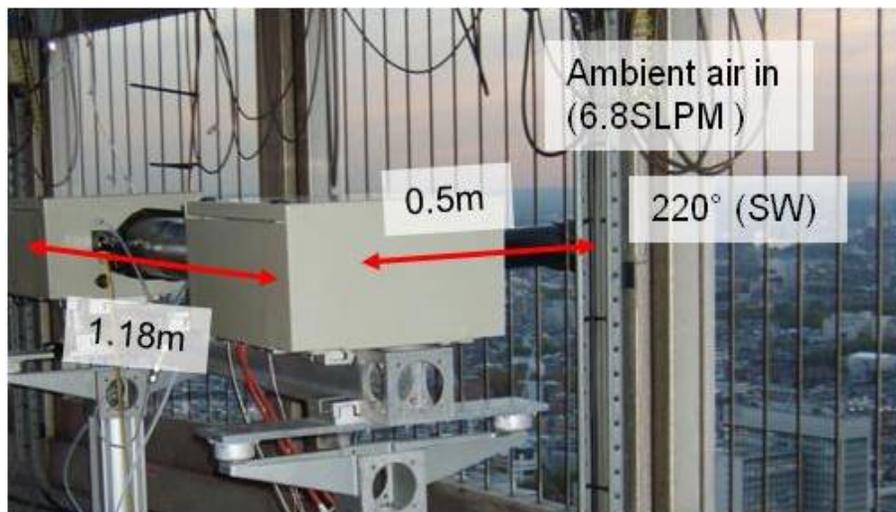
Fig. 2. The LED-BBCEAS setup on the balcony of level T35 of the BT Tower, London.
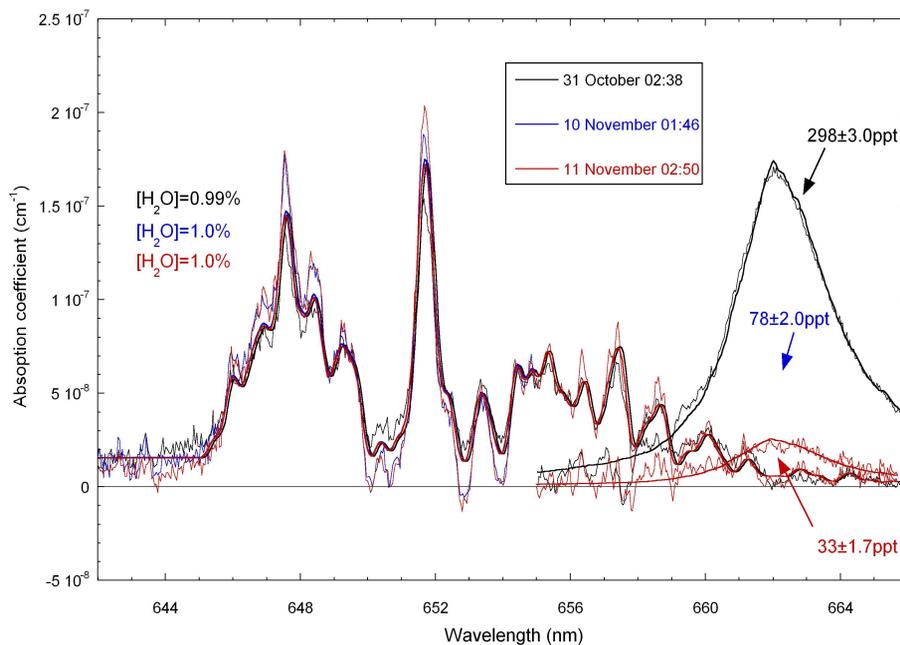
Fig. 3. Three example 15s absorption spectra from REPARTEE-II depicting the NO_3 absorption feature at 662 nm and the polyad vibrational overtones of water vapour. Features from the same spectrum are coded by colour and dated as indicated on the plot. Derived $NO_3+N_2O_5$ mixing ratios by volume as indicated on plot take into account different mirror R values but are prior to inclusion of the inlet loss conversion factor. Absorption coefficient=0 line shown for clarity.
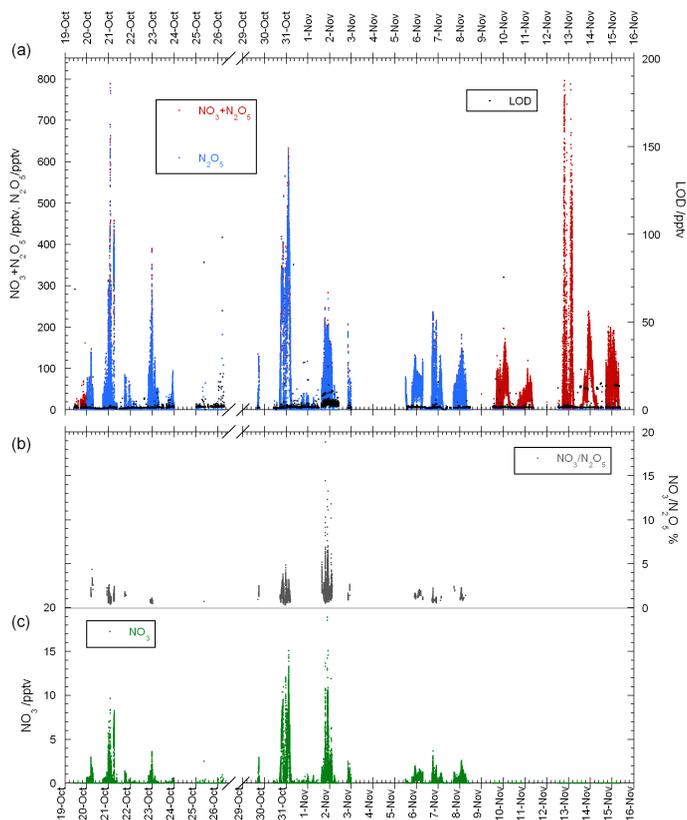
Fig. 4. LED-BBCEAS measurements of mixing ratios of $NO_3+N_2O_5$ (Panel **(a)**, red) from the REPARTEE-II campaign. All raw data (15s acquisitions) shown. A quantifiable measurement exists for all times where a LOD (Panel **(a)**, black) is shown. Data partitioned into N_2O_5 (Panel **(a)**, blue) and NO_3 (Panel **(c)**, green) where required ancillary data (NO_2 and ambient temperature) is available. Panel **(b)** (grey) shows NO_3/N_2O_5 ratio in %.
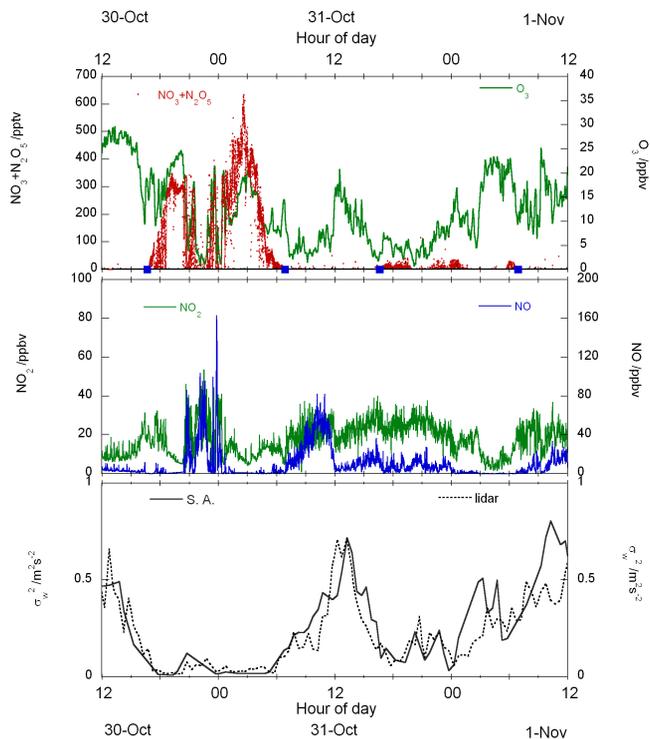
Fig. 5. A detailed plot of the continuous dataset of chemical and physical observations from 12:00 LT (noon) on 30 October to 12:00 LT on 1 November 2007. The top panel shows mixing ratios of $NO_3+N_2O_5$ (red) that are greater than the LOD of ~2 pptv, (not shown), (temporal resolution=15 s), O_3 mixing ratios (green) (temporal resolution=5 min) and approximate sunrise and sunset (blue squares). The middle panel shows mixing ratios of NO (green) and NO_2 (blue), (temporal resolution=1 min). The bottom panel shows the variance of w (σ_w^2), (temporal resolution=1 h) the vertical velocity component, as measured by the Doppler lidar and ultrasonic anemometer on the BT tower. (See text for measurement details).
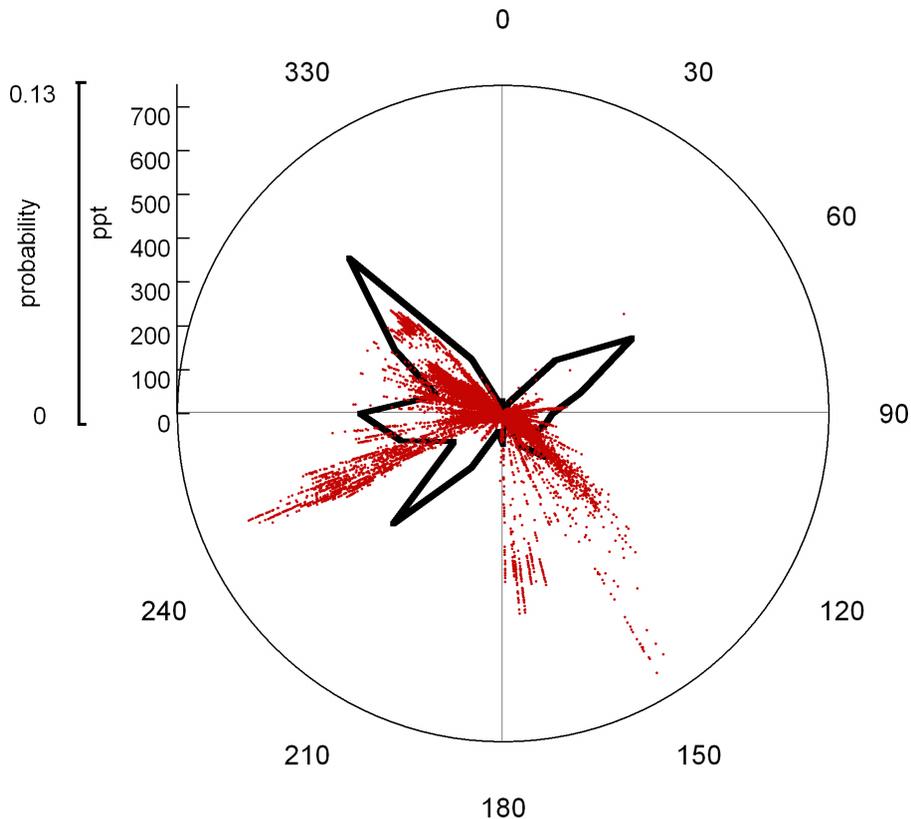
Fig. 6. Wind direction (by origin) plot of $NO_3+N_2O_5$ (hourly mean) with wind direction probability, binned into 20° regions by origin (black line), during times when BBCEAS measurements were made and an LOD reported during REPARTEE-II.
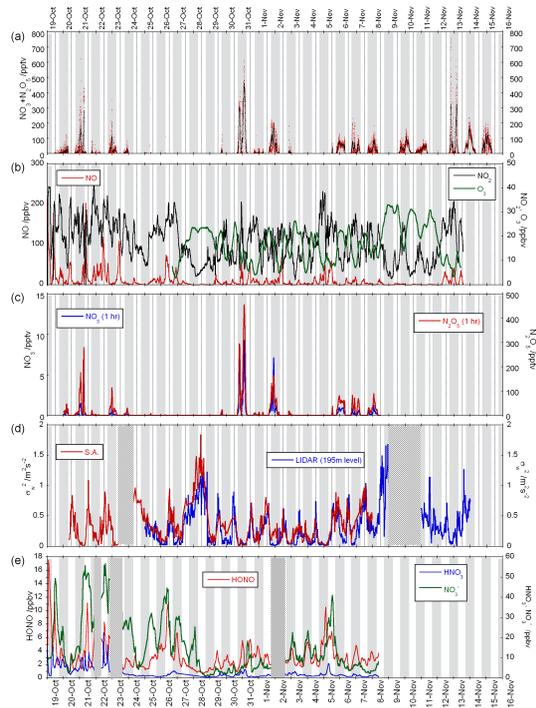
Fig. 7. A summarised time series of measurements during REPARTEE-II. **(a)** LED-BBCEAS retrieved $NO_3+N_2O_5$ (red points), 1 h moving mean (black line). **(b)** Mixing ratios of NO, NO_2 and O_3; **(c)** Hourly mean mixing ratios of NO_3 and N_2O_5 as inferred from measurements in panels **(a)** and **(b)**. Panel **(c)** Depicts the standard deviation of the vertical velocity variance (σ_w^2), a measure of turbulence in the vertical direction, as indicated by nearby lidar measurements (see text) at its nearest vertical level of 195 m, and by the ultrasonic anemometer (SA) above the tower. Panel **(e)** shows nitrous acid (HONO), nitric acid (HNO_3) and nitrate aerosol (NO_3^-) mixing ratios for comparison. Hatched areas depict no measurement.
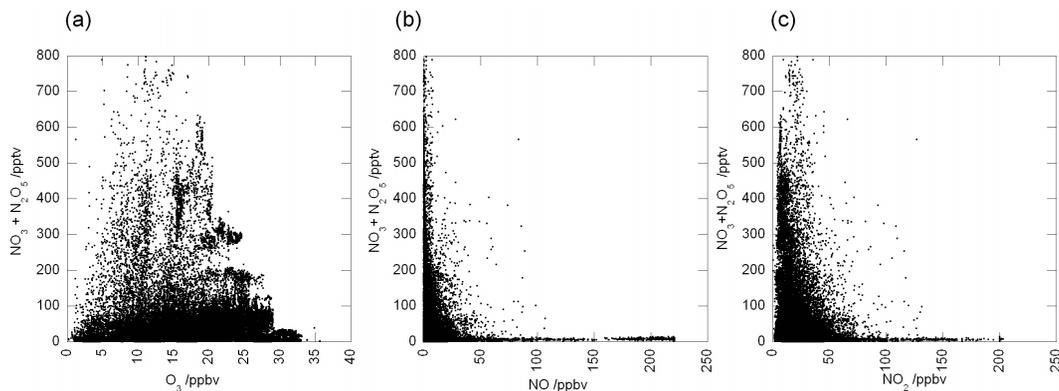
Fig. 8. Scatter plots showing correlation of mixing ratios of $NO_3+N_2O_5$ against **(a)** O_3, **(b)** NO and **(c)** NO_2 for all night-time data. Data for species on horizontal axis was interpolated (within 10 min where available, otherwise not shown) onto same time-grid as $NO_3+N_2O_5$.
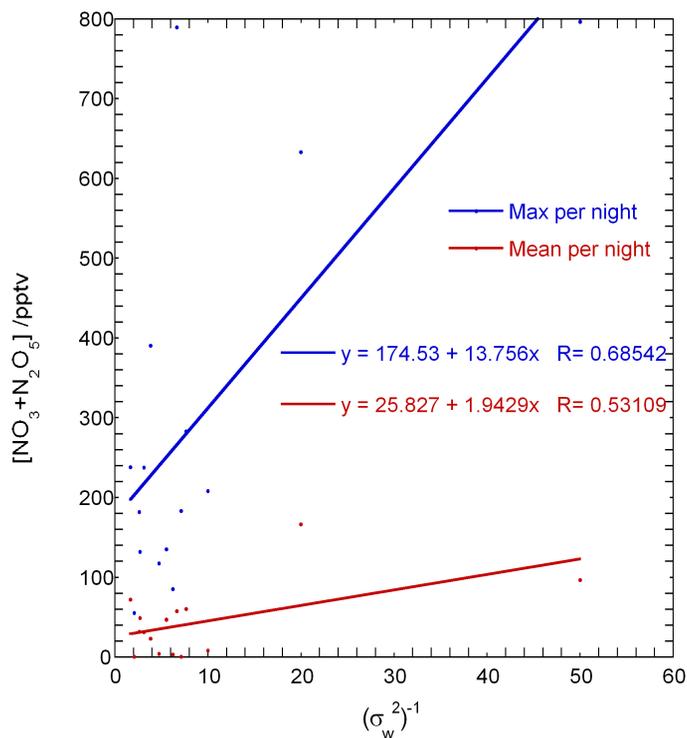
Fig. 9. Correlation plots of the reciprocal of the mean night-time standard variance of the vertical velocity (σ_w^2) against maximum (blue) and mean (red) $NO_3 + N_2O_5$ mixing ratio per night during REPARTEE-II. Vertical variance data matched onto BBCEAS time-stamp. Night-time as defined by local sunrise/sunset times.
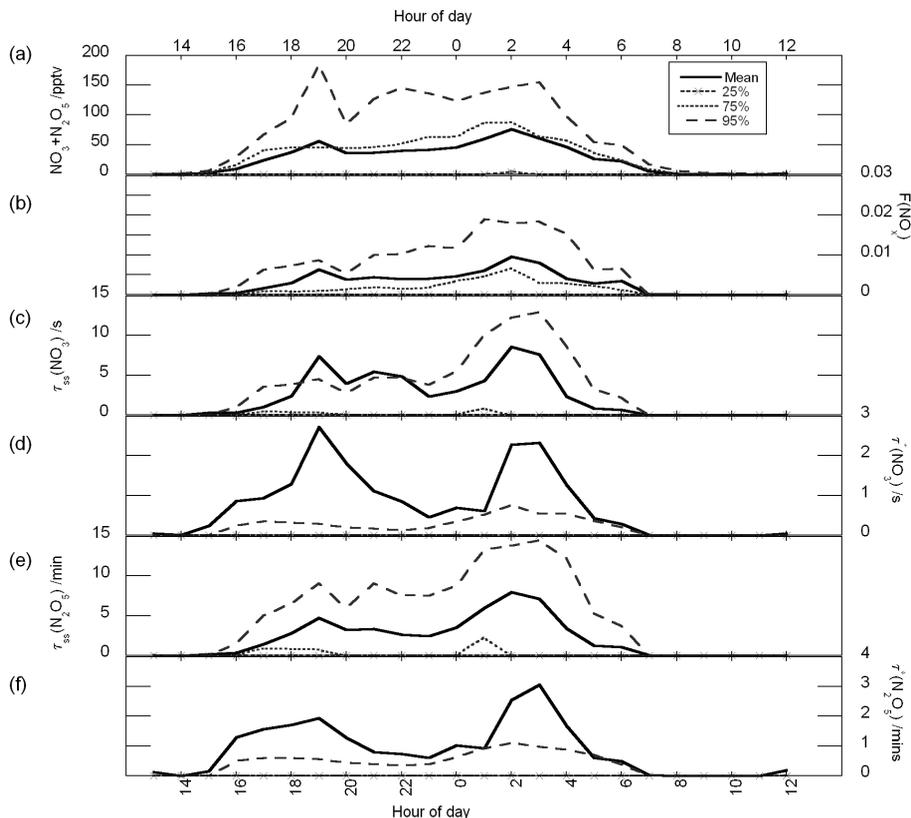
Fig. 10. Hourly average diurnal trend plots and their statistical ranges for **(a)** $NO_3+N_2O_5$ mixing ratios; **(b)** $F(NO_x)$; **(c)** $\tau_{ss}(NO_3)$/min and **(d)** non steady-state $\tau^*(NO_3)$/s; **(e)** $\tau_{ss}(N_2O_5)$/min **(f)** non steady-state $\tau^*(N_2O_5)$/min. For derivations of these values, see text. The large variability in both datasets is shown, as the mean being greater than the 95th percentile for much the non-steady-state treatment data. A shorter and more highly variable lifetime is determined by the non-steady state analysis.

Title Page

Abstract | Introduction

Conclusions | References

Tables | Figures

|◄ | ►|

◄ | ►

Back | Close
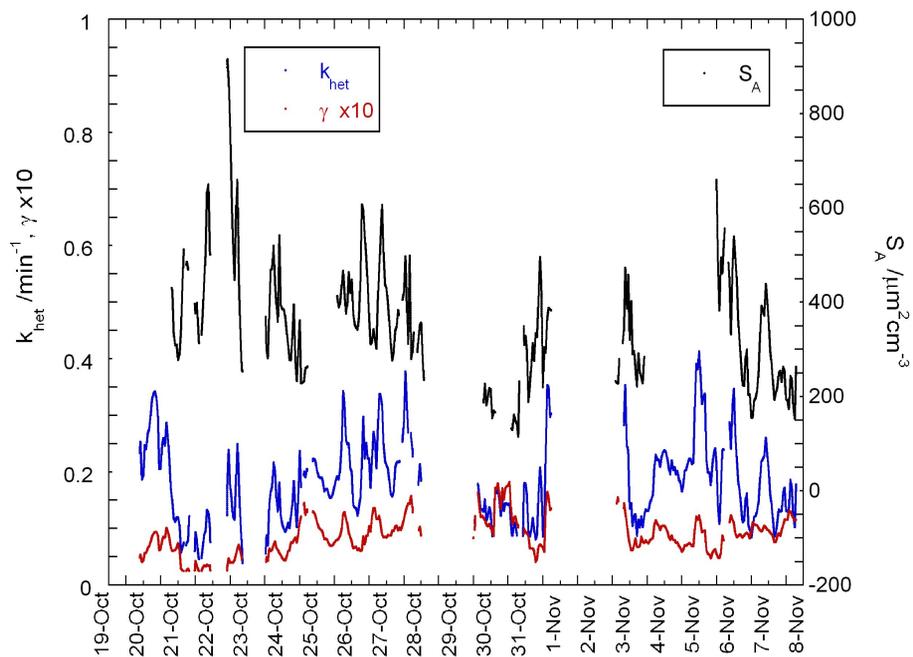
Full Screen / Esc

Fig. 11. Estimated parameters for the rate of uptake of N_2O_5 onto aerosols (R4). See text for details.